Responses of a thin flexible pavement loaded with tires of various dimensions and configurations

Shafiqur Rahman, Abubeker Ahmed & Sigurdur Erlingsson

Published online: 17 Apr 2025.

Submit your article to this journal ↗

Article views: 96

View related articles ↗

View Crossmark data ↗

Taylor & Francis
Taylor & Francis Group

🔓 OPEN ACCESS | Check for updates

Responses of a thin flexible pavement loaded with tires of various dimensions and configurations

Shafiqur Rahman[a], Abubeker Ahmed[a] and Sigurdur Erlingsson[a,b]

[a]Pavement Technology, Swedish National Road and Transport Research Institute (VTI), Linköping, Sweden; [b]Faculty of Civil and Environmental Engineering, University of Iceland, Reykjavik, Iceland

ABSTRACT

This study examines pavement responses under six tire types: two conventional duals, one conventional single, two first-generation widebase (FGWB) and one new-generation wide-base (NGWB) tire. Full-scale accelerated testing using a Heavy Vehicle Simulator measured stresses and strains in pavement layers under varying wheel loads, inflation pressures and lateral wander. Tire footprints were also recorded. Single tires caused higher strains in the asphalt concrete layer and greater stresses in unbound layers than dual tires, increasing the risk of fatigue cracking and permanent deformation. Among single tires, the NGWB 455/55R22.5 caused the least damage, while the FGWB 425/65R22.5 caused the most. Damage ratios showed that single tires were considerably more damaging than duals, depending on load and damage type. Increased load consistently raised stress and strain levels. However, inflation pressure effects varied: NGWB and dual tires showed decreased pavement responses with higher pressure, while other tires showed the opposite trend.

Introduction

Tire-pavement interaction plays a fundamental role in pavement engineering, as vehicle loads are transmitted through tires into the pavement structure. However, this interaction is complex, as the resulting stresses depend on various tire properties, including inflation pressure, dimensions, tread pattern, and material characteristics. Additionally, the rolling motion of the wheel further influences stress distribution.

Various tire dimensions and configurations, including single and dual tires, are used across different vehicle types, significantly influencing pavement damage (Al-Qadi et al., 2000; Al-Qadi et al., 2004; COST334, 2001; De Beer et al., 2004). Proper selection of tire configurations can minimise pavement degradation by distributing loads more effectively and reducing critical stresses and strains. To improve load distribution and minimise pavement stress, dual tires have been widely used in heavy-duty trucks for about a century, offering advantages such as enhanced control, weight distribution, and load capacity. Their larger contact area helps distribute axle loads, reducing stress and strain on the pavement. However, a major drawback of dual tires is reduced fuel efficiency. In response, the tire industry has sought to optimise tire dimensions and configurations to improve fuel economy, load capacity, safety, and durability (Fedujwar & Sahoo, 2023; Liu et al., 2024). One such development was the introduction of first-generation wide-base (FGWB) tires (385/65R22.5 and 425/65R22.5) in the early 1980s (Wang & Roque, 2011). These tires featured wider treads than conventional single wheels

---

and were preferred over dual tires for several reasons: they were lighter, improving fuel efficiency; they required simpler pressure maintenance; they provided a lower centre of gravity, enhancing ride quality; and they generated less scrap due to reduced sidewall area. However, despite these benefits, FGWB tires were found to increase pavement damage due to higher contact stresses (Al-Qadi & Wang, 2009; Greene et al., 2010; Moazami et al., 2011; Saevarsdottir et al., 2016; Wang & Roque, 2011; Wiman, 2006; Wiman & Erlingsson, 2008). To address these issues, a new generation of wide-base (NGWB) tires (445/50R22.5 and 455/55R22.5) was introduced in the early 2000s (Al-Qadi et al., 2018; Al-Qadi & Wang, 2012; Wang & Roque, 2011). These tires provided a larger pavement contact area, potentially reducing pavement damage. Xue et al. (2015, 2016) conducted field investigations by measuring horizontal tensile strain at the bottom of the asphalt layer under different tire types. Their findings indicated that NGWB tires exhibit performance comparable to or even more road-friendly than conventional dual-tire assemblies. Similar results were reported by Saliko and Erlingsson (2021, 2023) based on strain and stress measurements from instrumented in-service road structures. However, further research is needed to fully assess their long-term impact on pavement performance.

Researchers have employed various approaches to study tire-pavement interaction. Some have focused on measuring direct contact interaction to develop interaction models (Gong et al., 2023; Zhao & Wang, 2022), while others have used numerical simulations to predict contact behaviour (Bai et al., 2021; Manyo et al., 2021; Wang et al., 2012; Wollny et al., 2016; Xie & Yang, 2019; Zheng et al., 2022). Additionally, some studies have combined modelling and experimental investigations (Al-Qadi et al., 2018; Fedujwar & Sahoo, 2023; Greene et al., 2010). However, many of these analyses have been theoretical, often overlooking the impact of moving traffic loads. Furthermore, only a limited number of studies have utilised sensor-based measurements from instrumented pavements to assess the effects of heavy vehicles with different tire types.
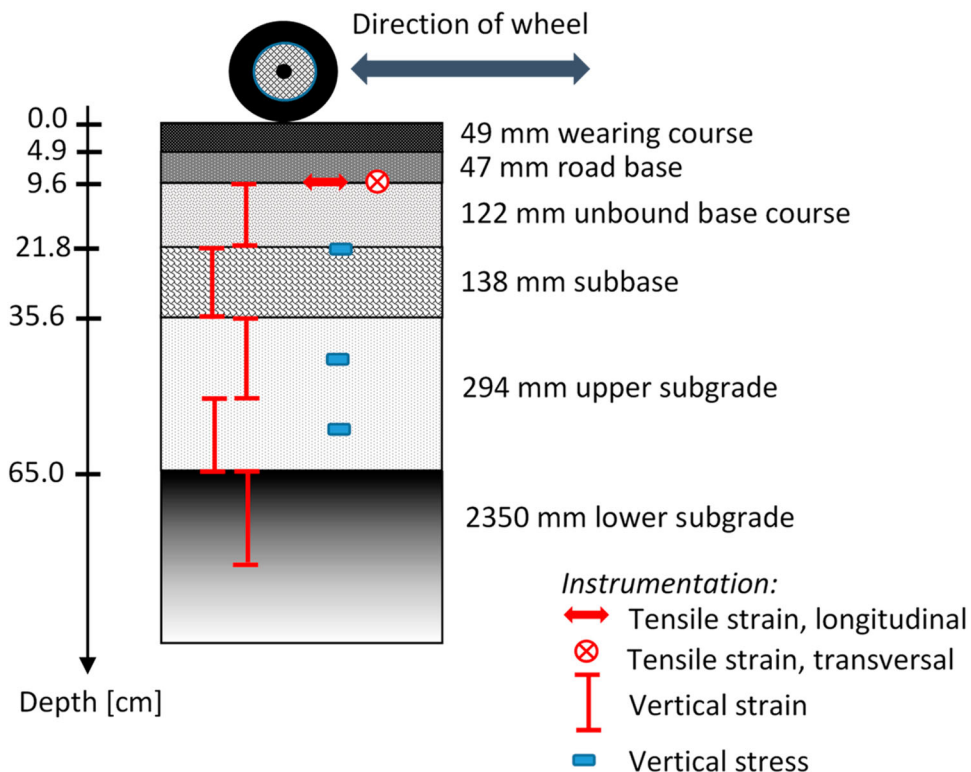

Figure 1. The test structure and instrumentation (longitudinal section).

This study aims to evaluate the impact of various tire types and configurations on pavement performance through full-scale measurements. This involved accelerated testing of an instrumented thin pavement structure using a Heavy Vehicle Simulator (HVS) in a climate-controlled environment. The tire types investigated included two conventional dual tire assemblies (275/80R22.5 and 295/80R22.5), one conventional single tire (315/80R22.5), two FGWB tires (385/65R22.5 and 425/65R22.5), and one NGWB tire (455/55R22.5). The stress and strain responses of the different layers of the pavement structure were analysed under dynamic loading with these tires, considering various combinations of wheel loads and inflation pressures. This article presents an extended analysis based on a previous study by Ahmed et al. (2018).

The test procedure

A thin pavement structure was instrumented in various layers and the responses of the layers were measured when loaded with various tires using an HVS.

The test structure

A thin asphalt pavement structure was used in this study. The test structure was composed of five layers, namely, asphalt concrete (AC) wearing course having a nominal maximum aggregate size of 16 mm and 70/100 pen grade bitumen, bituminous base course layer having a nominal maximum aggregate size of 22 mm and pen grade bitumen of 160/200, unbound crushed rock base, sub-base and fine sand subgrade over a stiff underlying structure. The pavement structure was first loaded with

Table 1. Combinations of tire pressure and wheel load investigated.

Tire pressure (kPa)	Wheel load (kN)			
700	40	50	60	–
800	40	50	60	80
900	40	50	60	80
950	–	50	–	–

Figure 2. Photograph of the tires.

Table 2. Tire dimensions and configurations.

Designation	Dimensions	Configuration	Range of half axle loads (kN)	Range of tire pressures (kPa).
S315	315/80R22.5	Single	40–80	700–950
S385	385/65R22.5	Single	40–80	700–950
S425	425/65R22.5	Single	40–80	700–950
S455	455/40R22.5	Single	40–80	700–950
D275	275/80R22.5	Dual	40–80	700–950
D295	295/80R22.5	Dual	40–80	700–950

Table 3. Measurements of the tire-pavement contact surface.

		S315			S385			S455			D295		
Wheel load (kN)	Tire pressure (kPa)	Width (mm)	Length (mm)	Total area (mm^2)	Width (mm)	Length (mm)	Total area (mm^2)	Width (mm)	Length (mm)	Total area (mm^2)	Width (mm)	Length (mm)	Total area (mm^2) (both tires)
40	700	256	267	49047	304	237	49928	379	208	67864	–	–	–
	800	256	257	46203	304	223	47294	378	194	62293	–	–	–
	900	–	–	–	305	225	48143	376	188	60206	–	–	–
50	700	256	308	56505	–	–	–	382	227	76741	193	254	71380
	800	256	287	53292	–	–	–	381	214	72005	–	–	–
	900	–	–	–	–	–	–	–	–	–	194	239	63320
	950	256	274	51410	–	–	–	–	–	–	–	–	–
60	700	256	363	64790	305	322	67742	385	264	88459	–	–	–
	800	255	341	61405	305	293	63629	384	237	82509	–	–	–
	900	–	–	–	306	287	63860	383	228	78306	–	–	–
80	800	257	402	72425	305	359	75742	386	292	97380	–	–	–
	900	–	–	–	307	351	76398	386	274	92257	–	–	–

Note: – = data missing

one million standard axles, with a normally distributed lateral wander from a dual tire assembly. Consequently, all post-compaction was completed, and the pavement could be considered an intact, old pavement structure without any visible distress on the surface.

The test structure was instrumented to measure the structural responses. Asphalt strain gauges (ASG) were used to measure the longitudinal and transverse horizontal strains at the bottom of the AC layer. EMU (strain measuring units) coils were employed to measure the vertical strains in the unbound base, subbase and subgrade layers. The vertical stresses in the subbase and subgrade layers were measured using soil pressure cells (SPC). Figure 1 shows the cross section of the test structure and the instrumentations. Detailed information about the instrumentation can be found in Saevarsdottir et al. (2016).

Full-scale tests

Full-scale accelerated pavement tests were conducted using an HVS (Wiman, 2006; Wiman & Erlingsson, 2008). The tests were carried out in an indoor concrete test pit, 15 m in length, 5 m wide and 3 m deep. A climate chamber was used in order to keep controlled environmental conditions where the temperature was maintained at 10°C (yearly average temperature considered as standard for Swedish road design and analysis). In the HVS, loading can be applied through either single or dual wheels (Saevarsdottir et al., 2016 Wiman & Erlingsson, 2008). The tests were conducted at a constant speed of 12 km/h. Various numbers of sensors of each type were installed at each location as shown in Figure 1. The sensors were placed along the central vertical plane of the structure. After mounting each wheel, measurements were carried out as it travelled back and forth along a 6 m line on the surface of the structure. To account for the lateral wander of traffic, the wheels' lateral positions were shifted after every back-and-forth movement (10 passes along each line) in steps of 5 cm up to 25 cm of both sides of the centre line. It should be noted that the study was carried out for isolated wheels eliminating interference from any other wheels.

The tire inflation pressures were 700, 800, 900 and 950 kPa. For the different tire pressures, the wheel load was increased in steps from 40 to 80 kN. The matrix of the combination of tire inflation pressure and wheel load is shown in Table 1.
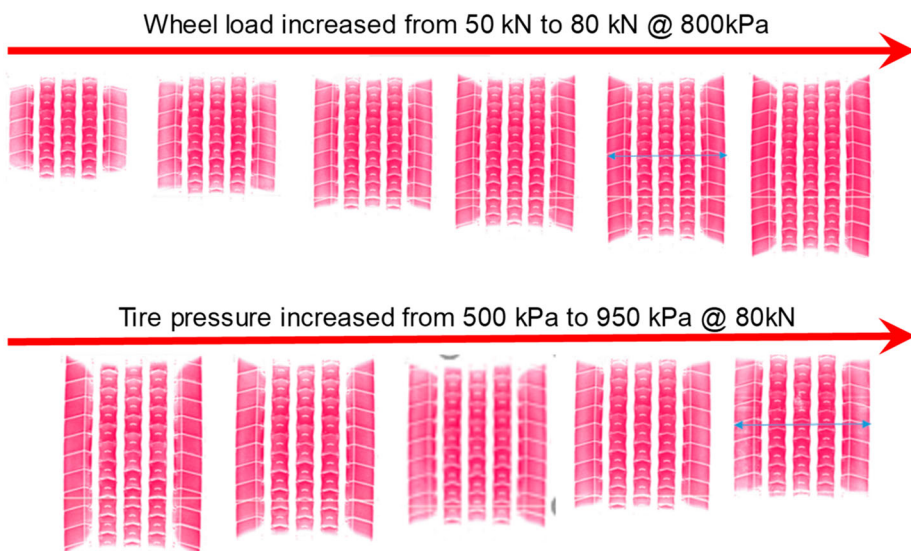

Figure 3. Footprints of the tire S315 as a function of wheel load and inflation pressure (Said et al., 2020).

A total of six types of tires were investigated, two conventional dual tire assemblies, one conventional single tire, two FGWB tires and one NGWB tires. The dimension of the tires, the range of applied wheel loads and corresponding tire inflation pressures are presented in Table 2. Figure 2 shows a photograph of those tires.

Tire footprint measurement

The contact area between the different tires and the pavement surface (AC wearing course) was measured in static condition using a pressure sensitive film (Said et al., 2020). The impact of wheel load and tire inflation pressure on the contact area was studied by taking measurements at various load

(a) Transverse strain (bottom of the AC layer)
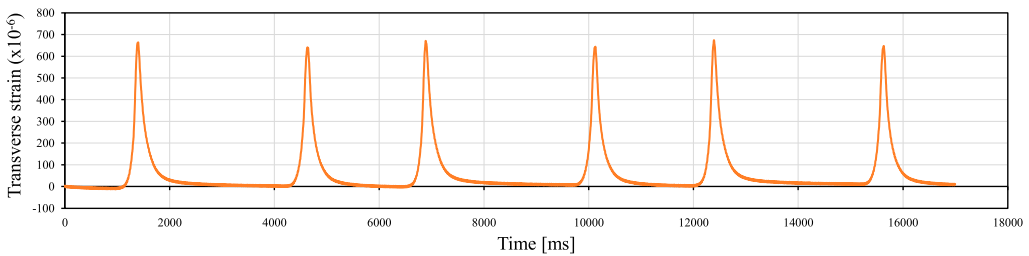
(b) Longitudinal strain (bottom of the AC layer)
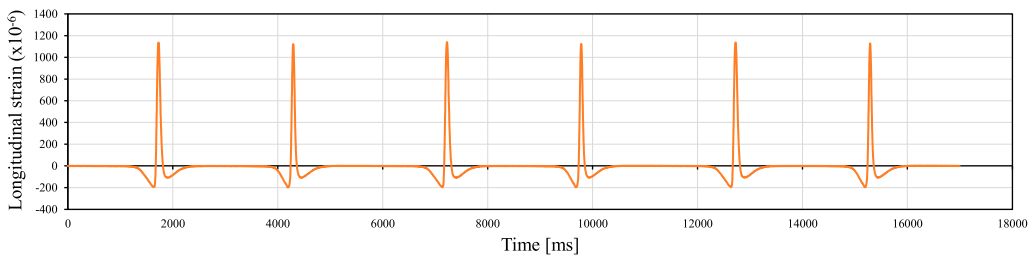
(c) Vertical strain (Base layer)
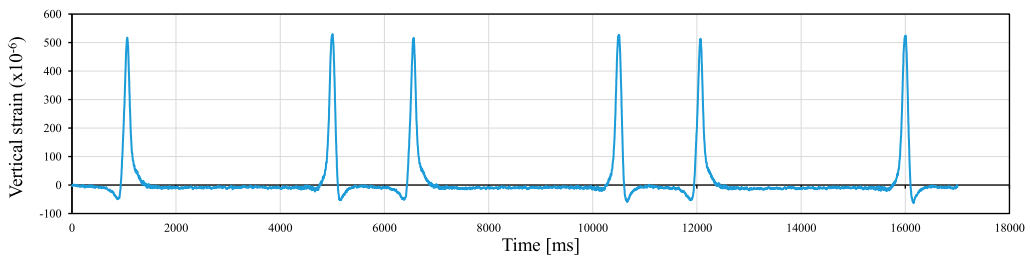
(d) Vertical stress

Figure 4. Typical registrations of the different sensors for the tire S455 (wheel load 50 kN, inflation pressure 800 kPa): (a) transverse horizontal strain, (b) longitudinal horizontal strain, (c) vertical strain in the base layer, and (d) vertical stresses at different depths.

levels and inflation pressures. Figure 3 shows the footprints of the conventional single tire S315 for increasing loads and inflation pressures. It should be noted that the footprints do not represent the pressure variations within the contact areas. The measured dimensions of the footprints are presented in Table 3. From Figure 3 and Table 3, it is apparent that for a specific inflation pressure, the contact area increases with increased load. The width of the contact area approximately remains equal to the width of the tire. With increased load, the length increases in the peripheral direction. On the other hand, for a certain wheel load, the contact area decreases with increased inflation pressure where the width of the area remains almost equal to the width of the tire. These observations and measurements are expected to explain the differences in the responses of the pavement structure loaded with different types of tires.

(a) Transverse strain (bottom of the AC layer)

(b) Longitudinal strain (bottom of the AC layer)
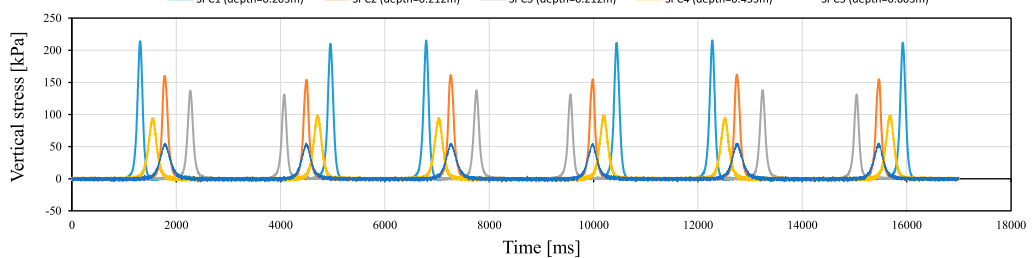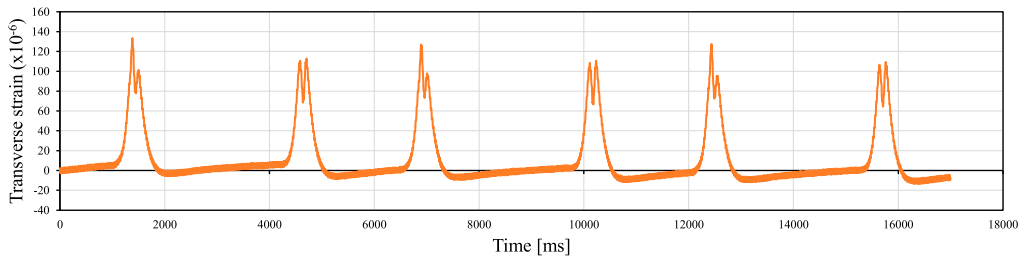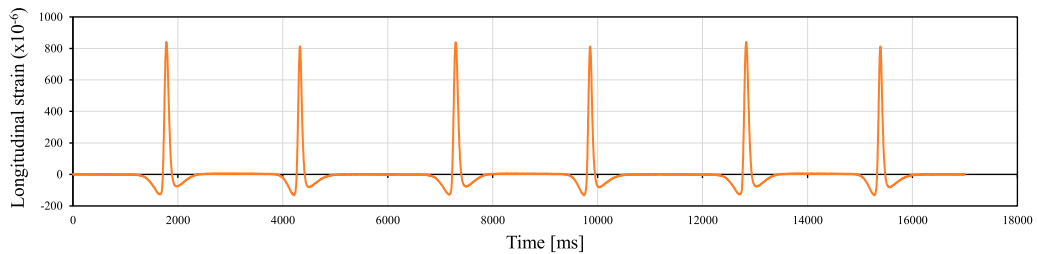

(c) Vertical strain (Base layer)
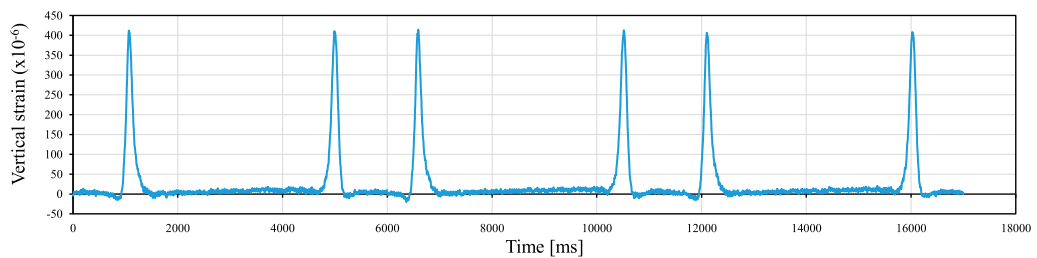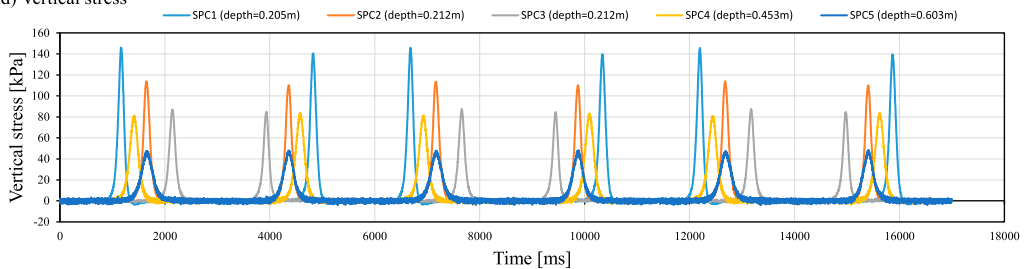
(d) Vertical stress

Figure 5. Typical registrations of the different sensors for the tire D295 (wheel load 50 kN, inflation pressure 800 kPa): (a) transverse horizontal strain, (b) longitudinal horizontal strain, (c) vertical strain in the base layer, and (d) vertical stresses at different depths.

Measured responses and discussions

The registered responses (stresses and strains) of the structure during the passages of the different tires are presented here. The measurements were carried out for a different combinations of wheel loads and tire pressures. In this article, responses corresponding to the wheel load of 50 kN and tire pressure of 800 kPa are presented. For other combinations of wheel loads and tire pressures, the magnitudes of the responses varied but the relative rankings of the tires were the same.

Figure 6. (a) Transverse, and (b) longitudinal tensile strains at the bottom of the asphalt layer (wheel load of 50 kN and inflation pressure of 800 kPa).

Figures 4 and 5 show typical registrations of the different sensors for three back and forth passages of the S455 and D295 tires, respectively. Here, the wheel load was 50 kN and inflation pressure was 800 kPa. The responses in Figure 4 are for the S455 tire when it passed directly above the sensors. Figure 5 represents the responses when the sensors were along the centreline between the two tires of the D295 configuration. Multiple sensors were used to measure each type of response. For clarity, responses from some of the selected sensors are presented in the figures. However, for the calculations, the mean values of the readings from all the sensors (same types and same vertical locations) were used.

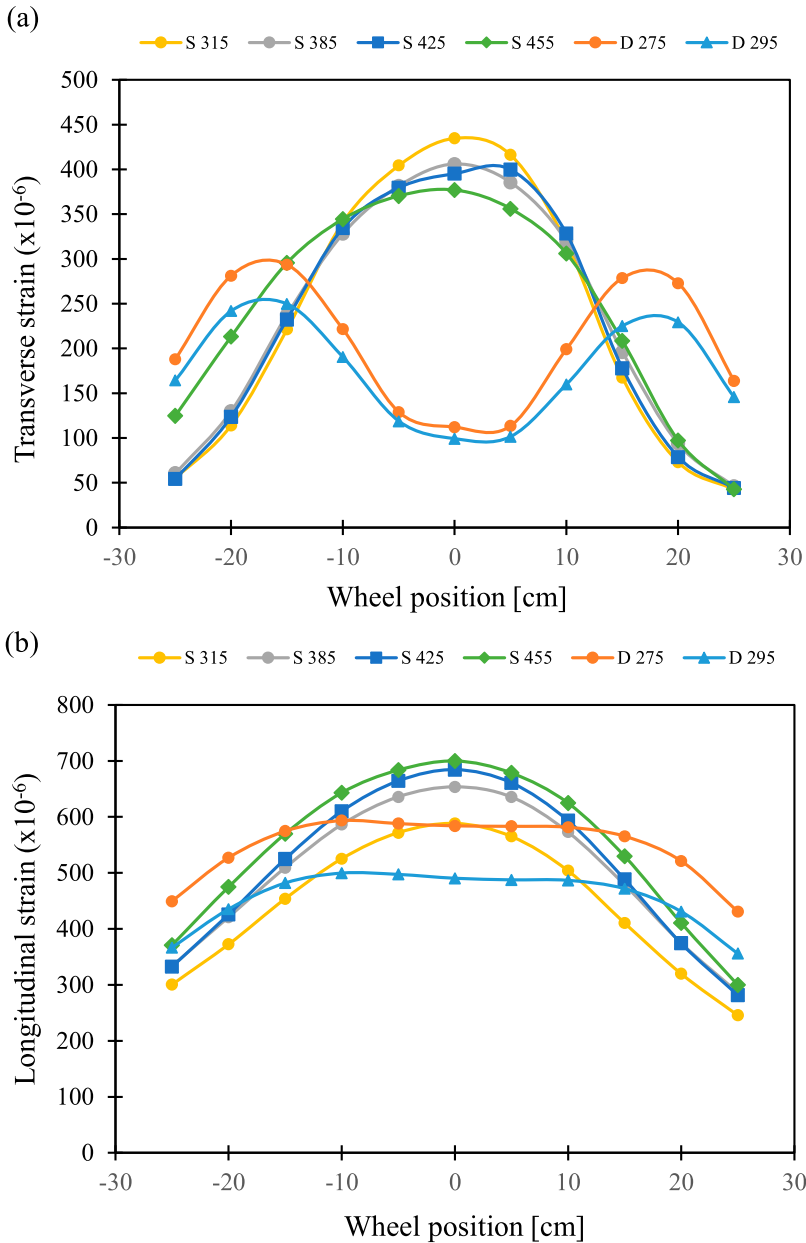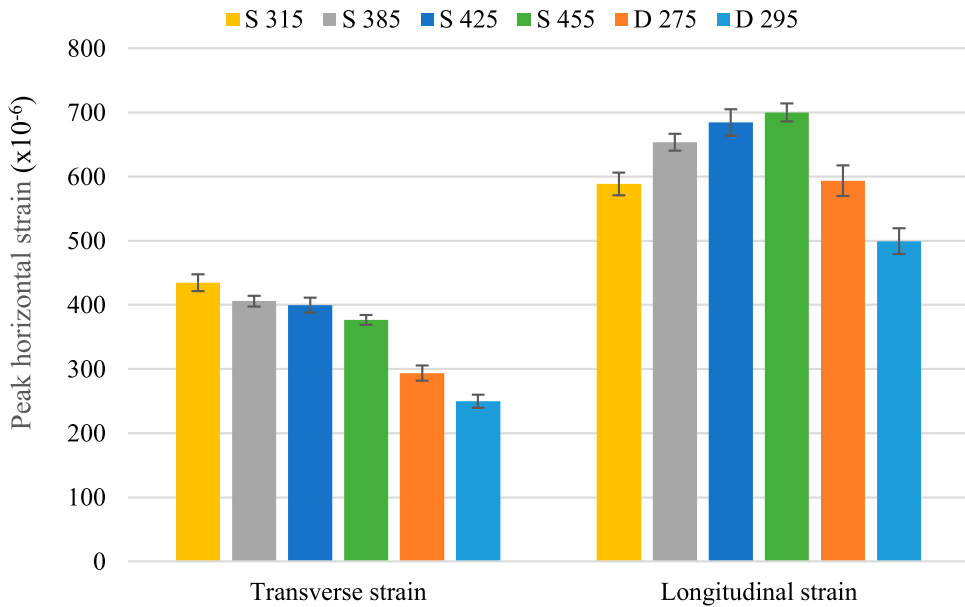**Figure 7.** Peak transverse and longitudinal tensile strains at the bottom of asphalt layer (wheel load of 50 kN and inflation pressure of 800 kPa).
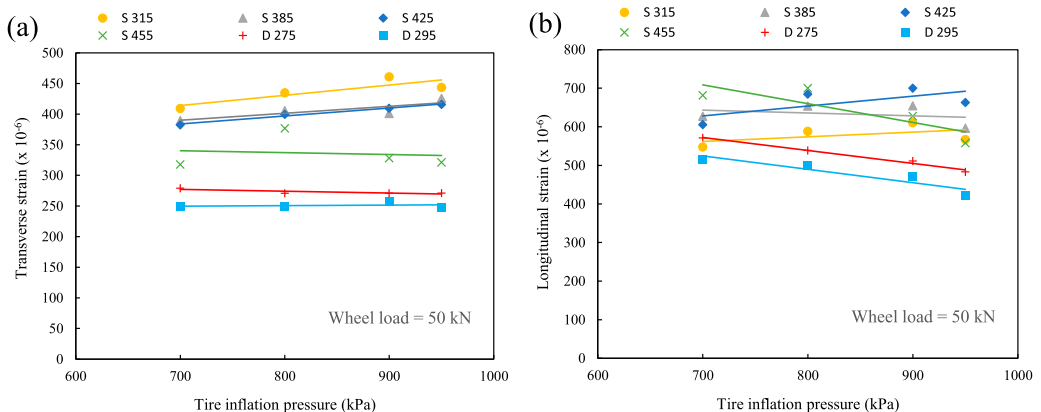

Figure 8. Peak transverse and longitudinal tensile strains at the bottom of AC layer with respect to tire inflation pressure.

Horizontal tensile strains at the bottom of the AC layer

The horizontal tensile strains at the bottom of the AC layer were measured using asphalt strain gauges (ASG). Measurements were registered both in the longitudinal (along the wheel path) and transverse directions (perpendicular to the wheel paths). Average registrations of these sensors for the various lateral positions of the wheels are shown in Figure 6. Figure 7 shows the peak strain values (regardless of lateral positions) corresponding to different tires.

From Figures 6 and 7, it is obvious that the single wheels tend to produce higher transverse strain at the bottom of asphalt layer compared to dual wheels. Of the single tires, the conventional single tire S315 produced the highest transverse strain and the lowest longitudinal strain and vice-versa for the widest single tire S455. It is apparent from Table 3 that for the same loading condition, as the width of the tire increases, the length of the contact area along the longitudinal direction decreases. Thus, it appears that the narrower dimension of the contact area induces higher horizontal strain along that direction. As the tensile strain at the bottom of the asphalt layer is associated with fatigue cracking, the use of single wheels may increase the risk of fatigue damage on thin asphalt pavements compared to dual wheels.

In Figures 6 and 7, the longitudinal strains are higher in magnitude than the transverse strain although the opposite trend was mentioned by Fedujwar and Sahoo (2023). This implies that there will be more transverse cracking than longitudinal cracking. However, in reality, longitudinal cracking is more common. One explanation may be that the tensile strain peak in the longitudinal direction is followed by immediate compressive strains (Figure 4(b)) that contribute to the healing of the AC layer.

In Figure 8, the effect of increased tire pressure on the transverse and longitudinal strains of the AC layer is shown. This figure shows that the transverse strains for the dual wheels and the S455 tire were not much affected by the inflation pressure. The other tires showed some increase in transverse strain with increased inflation pressure. On the other hand, the longitudinal strains decreased with

Figure 9. Peak transverse and longitudinal tensile strains at the bottom of asphalt layer with respect to wheel load.

Table 4. Damage ratios (*D*) of the different tires with respect to the D295 tire for fatigue cracking of the AC layer.

Tire pressure (kPa)	700			800				900				950
Wheel load (kN)	40	50	60	40	50	60	80	40	50	60	80	50
S315	8.9	7.3	6.8	10.8	9.2	7.9	7.0	12.3	10.2	9.2	7.7	10.4
S385	7.9	6.0	5.2	8.5	7.0	5.4	4.5	8.6	5.8	5.2	4.1	8.8
S425	6.8	5.6	5.0	8.5	6.6	5.5	4.5	9.4	6.4	5.8	4.5	8.0
S455	3.7	2.6	2.2	6.7	5.2	3.8	3.2	3.8	2.6	2.1	1.5	2.8
D275	1.8	1.6	1.6	1.1	1.9	1.3	1.3	1.1	1.2	1.3	1.2	1.4
D295	1.0	1.0	1.0	1.0	1.0	1.0	1.0	1.0	1.0	1.0	1.0	1.0

increased tire pressure for the dual wheels and the S455 wheel. The other tires showed slight increase in transverse strain with increased inflation pressure.

In Figure 9, the effect of increased wheel load on the transverse and longitudinal strains of the AC layer are shown. Here, for all cases, strains increased with increased wheel load.

To quantify and compare the different wheels for their risks of damaging the AC layer, the Asphalt Institute Method (Huang, 2004) was followed. According to this method, for any wheel, a relative damage ratio (*D*) compared to a reference wheel was calculated to assess the relative risk of damage by that wheel.
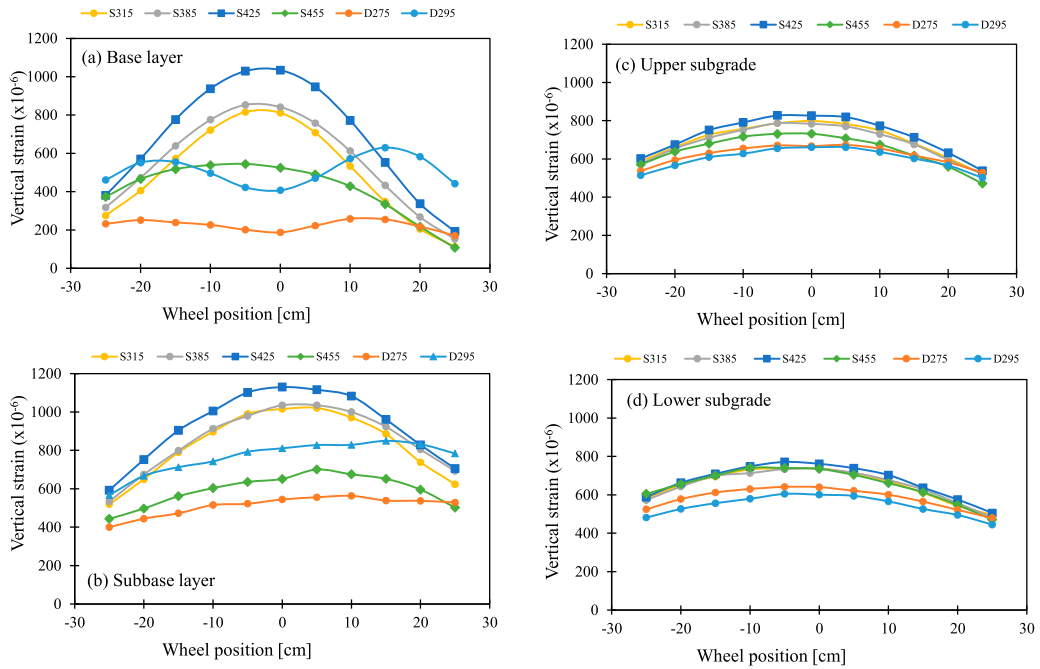
Figure 10. Vertical strains in the (a) base layer, (b) subbase layer, (c) upper subgrade, and (d) lower subgrade. The wheel load was 50 kN and the tire pressure was 800 kPa.
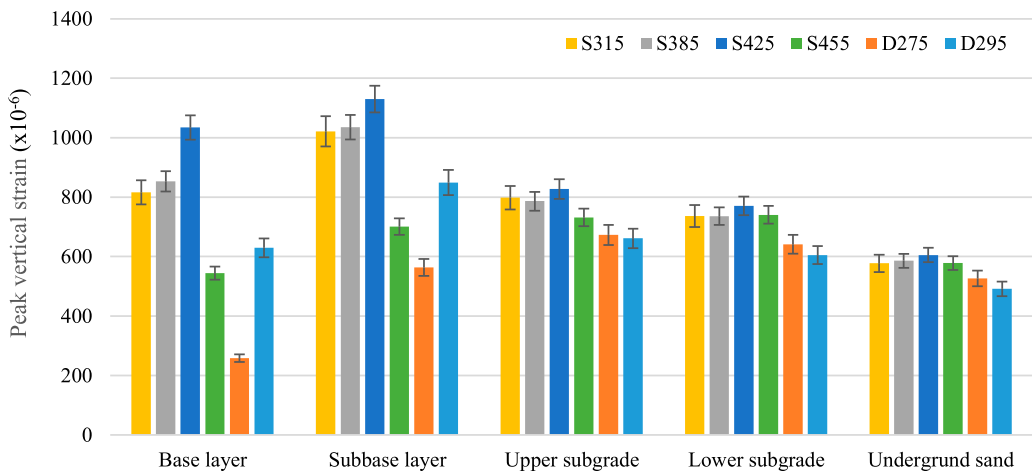
Figure 11. Peak vertical strains in the different layers. The wheel load was 50 kN and the tire pressure was 800 kPa.

According to the fatigue cracking of the AC layer criterion, the allowable number of load repetitions can be expressed as

$$N = a(\varepsilon)^b \tag{1}$$

where, N is the allowable number of load cycles, ε is the horizontal tensile strain at the bottom of the AC layer, a and b (b is usually taken as -4) are material constants. Then D can be defined as the ratio between the allowable number of load repetitions between a reference wheel and the wheel in
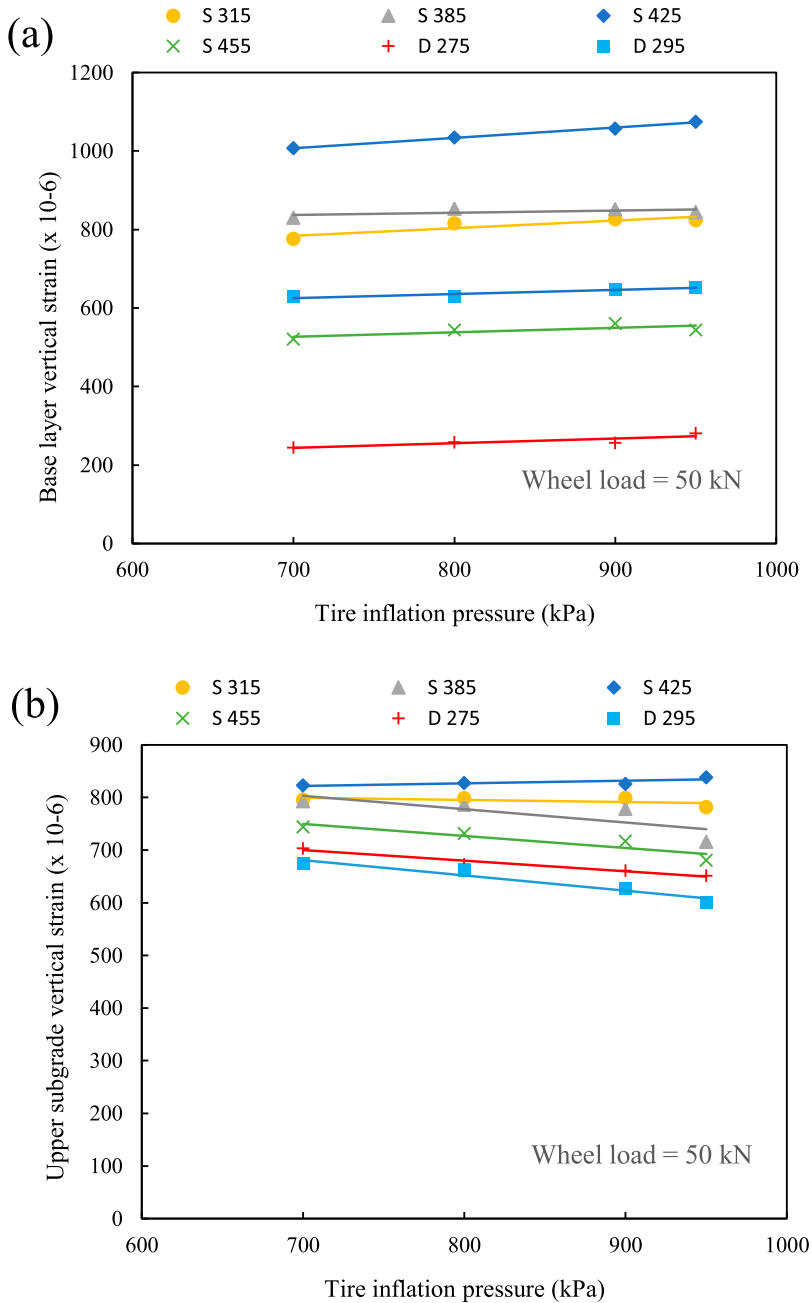

Figure 12. Peak vertical strains in (a) the baser layer, and (b) the upper subgrade with respect to inflation pressure.

consideration. In this study, the dual wheel D295 was considered as the reference since it was found to be the least damaging one. Thus, the damage ratios for the different wheels in relation to the D295 wheel were computed as:

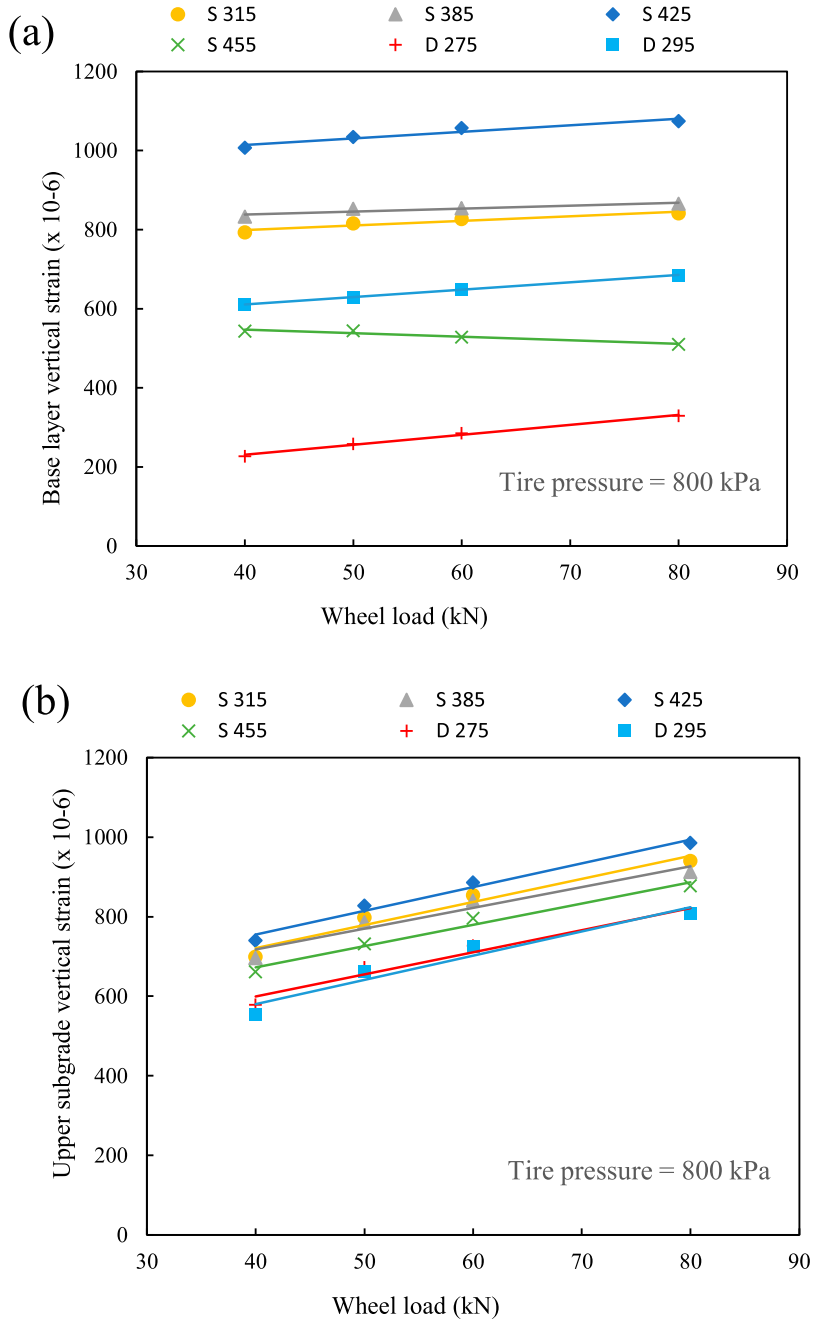$$D = \frac{N_{D295}}{N_t} = \left(\frac{\varepsilon}{\varepsilon_{D295}}\right)^4 \tag{2}$$

Figure 13. Peak vertical strains in (a) the baser layer, and (b) the upper subgrade with respect to wheel load.
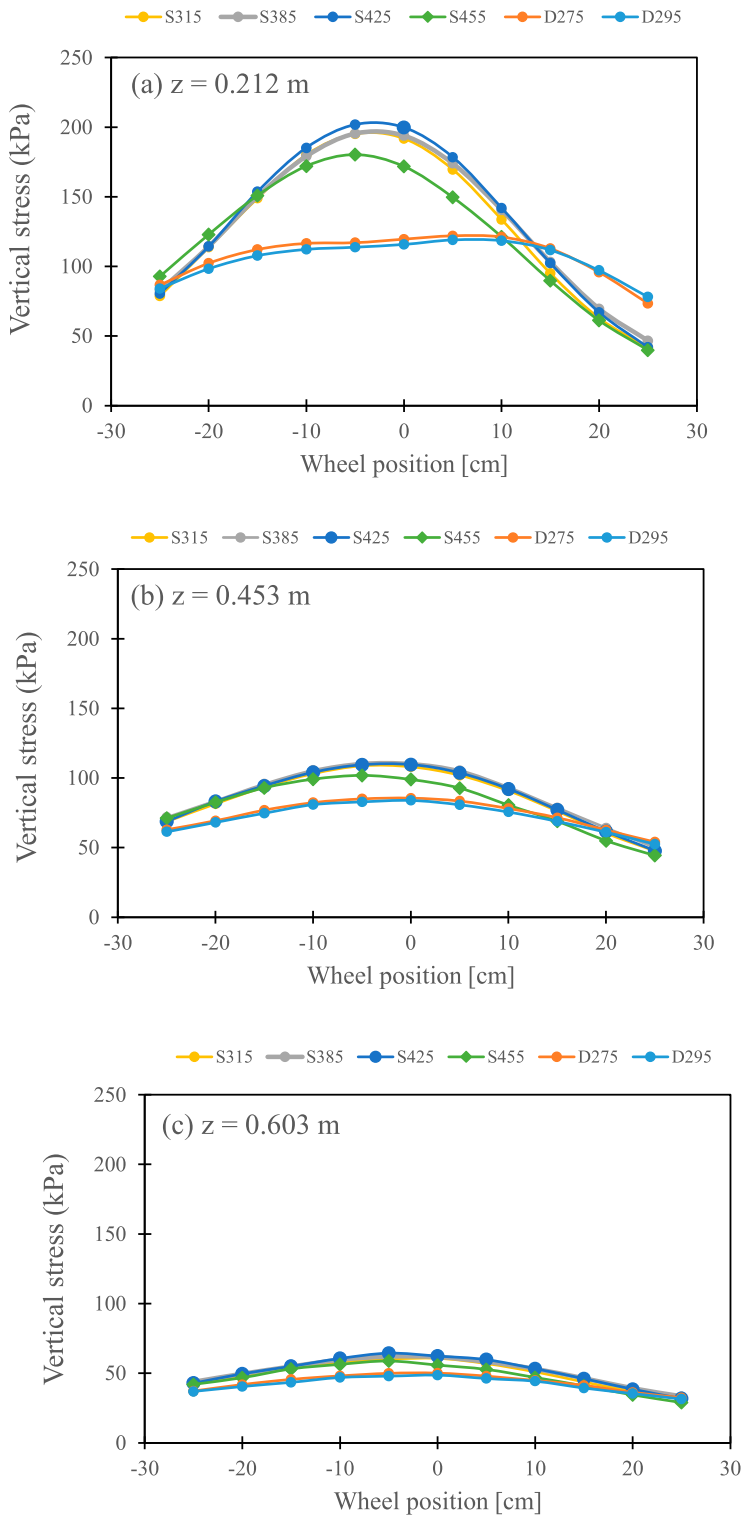
Figure 14. Vertical stresses at three vertical locations in the subbase and the upper subgrade.

where, N_{D295} and N_t are the allowable number of load repetitions for the D295 wheel and the wheel in question, respectively. ε_{D295} and ε are the horizontal tensile strain at the bottom of the AC layer for the D295 and the wheel in consideration, respectively. The calculated D values for the AC layer fatigue cracking in the longitudinal direction (transverse strain) are presented in Table 4. Here, the values of D represent how much more damaging the wheel in consideration is with respect to the wheel D295.

The numbers in Table 4 depict that, for AC fatigue cracking, the single wheels are several times (depending on wheel load and inflation pressure, the D values ranged from 1.5–12.3) more damaging than the dual wheels. However, the S455 wheel appears to be much less damaging than the other three single wheels for which the D values varied from 1.5–6.7. Among the single wheels, the S315 tire is the most damaging with D values between 6.8 and 12.3.

Vertical strain in unbound layers

The vertical strains in the base, subbase and subgrade were measured using three EMU coils per layer (Saevarsdottir et al., 2016). Average readings of these EMU coils for the different layers are presented in Figure 10. Figure 11 shows the peak strains caused by the different tires in the different layers, regardless of the lateral position. The figures show that the three single wheels (S315, S385 and S425) produced higher vertical strains in all layers than the dual wheels. However, the NGWB S455 tire produced vertical strains in the base and subbase layers that are close to those of the dual wheels. The FGWB S425 tire induced the highest strains in all cases. Other previous studies reported similar observations that FGWB tires are more damaging than dual tires and NGWB tires (Al-Qadi & Wang, 2009; Greene et al., 2010; Moazami et al., 2011). Hence, in this regard, the single tire S455 is as good as the dual tires. Consulting Table 3, it can be observed that for similar loading conditions, the S455 tire's

Table 5. Damage ratios (D) of the different tires with respect to the D295 tire for subgrade rutting.

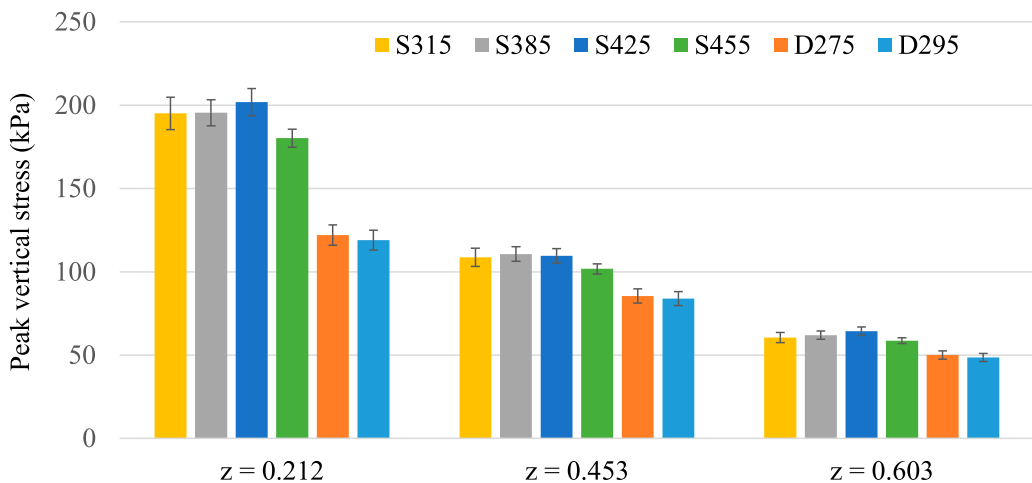| Tire pressure (kPa)	700			800				900				950
Wheel load (kN)	40	50	60	40	50	60	80	40	50	60	80	50
S315	2.3	1.9	2.1	2.5	2.1	1.9	1.8	3.0	2.6	2.4	2.0	2.9
S385	2.5	1.9	1.9	2.5	2.0	1.8	1.6	2.6	2.4	2.2	1.7	2.0
S425	2.7	2.2	2.3	3.2	2.5	2.2	2.2	3.7	3.0	2.8	2.3	3.8
S455	1.7	1.5	1.5	2.0	1.5	1.4	1.4	2.0	1.7	1.8	1.4	1.6
D275	1.4	1.2	1.1	1.2	1.1	1.0	1.0	1.2	1.2	1.2	1.0	1.4
D295	1.0	1.0	1.0	1.0	1.0	1.0	1.0	1.0	1.0	1.0	1.0	1.0

Figure 15. Peak vertical stresses at three vertical locations in the subbase and the upper subgrade.

contact areas are almost equal to those of the dual tires whereas the contact areas of the other single wheels are significantly smaller. Thus, the increased contact area of the S455 tire may be a contributing factor for the significantly lower vertical strains. However, the differences among the tires reduced with depth and the S455 tire behaved more like the single tires at greater depths. Hence, there is a greater risk of permanent deformation in the subgrade if the single wheels are used.
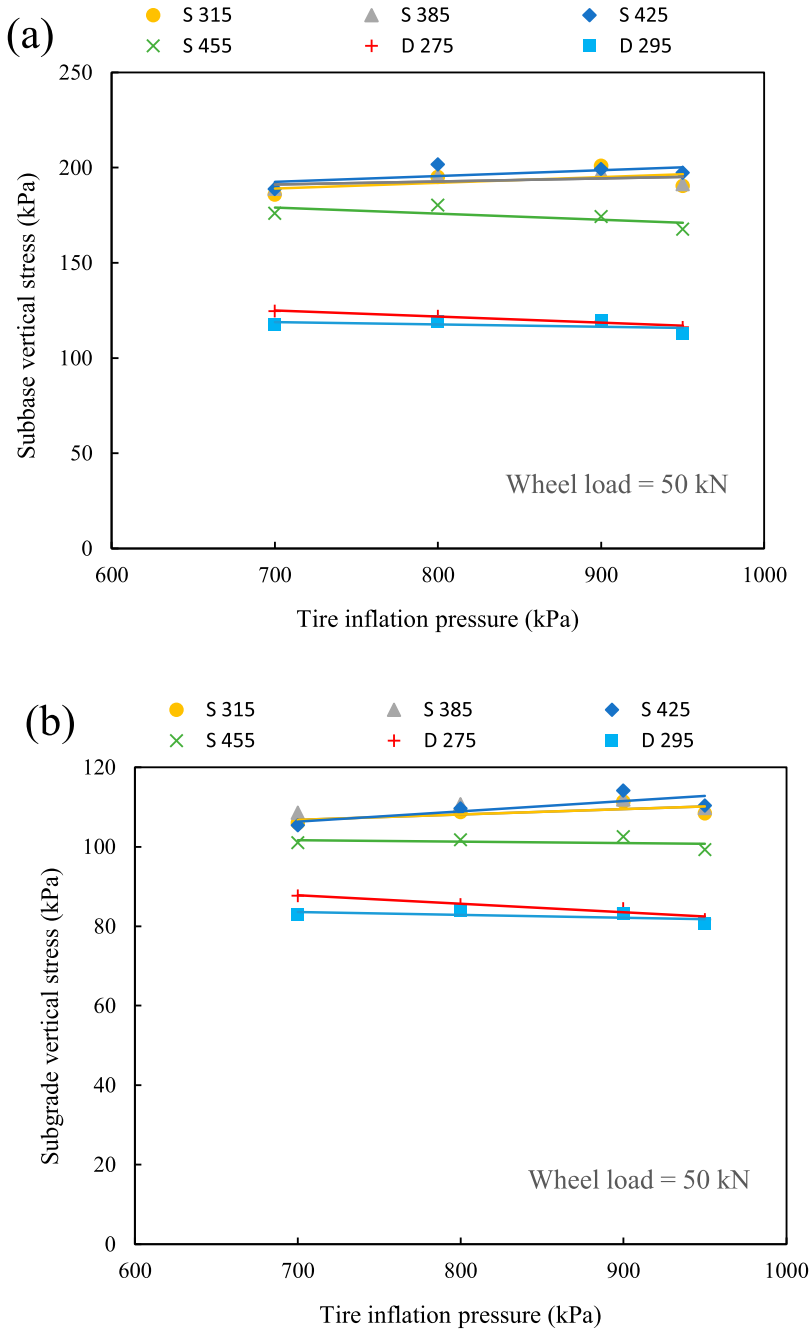

Figure 16. Peak vertical stresses at (a) the top of the subbase, and (b) the upper part of the subgrade with respect to tire inflation pressure.

Figure 12 shows the peak vertical strains in the base layer and the subgrade with respect to inflation pressure. It is seen that the strains in the base layer increased with increased inflation pressure. But the strains in the subgrade decreased with increased inflation pressure. In Figure 13, the increase in strains with increased wheel loads can be seen for the base and subgrade. Comparing the vertical strains in the base, the differences among the tires were much less in the subgrade.
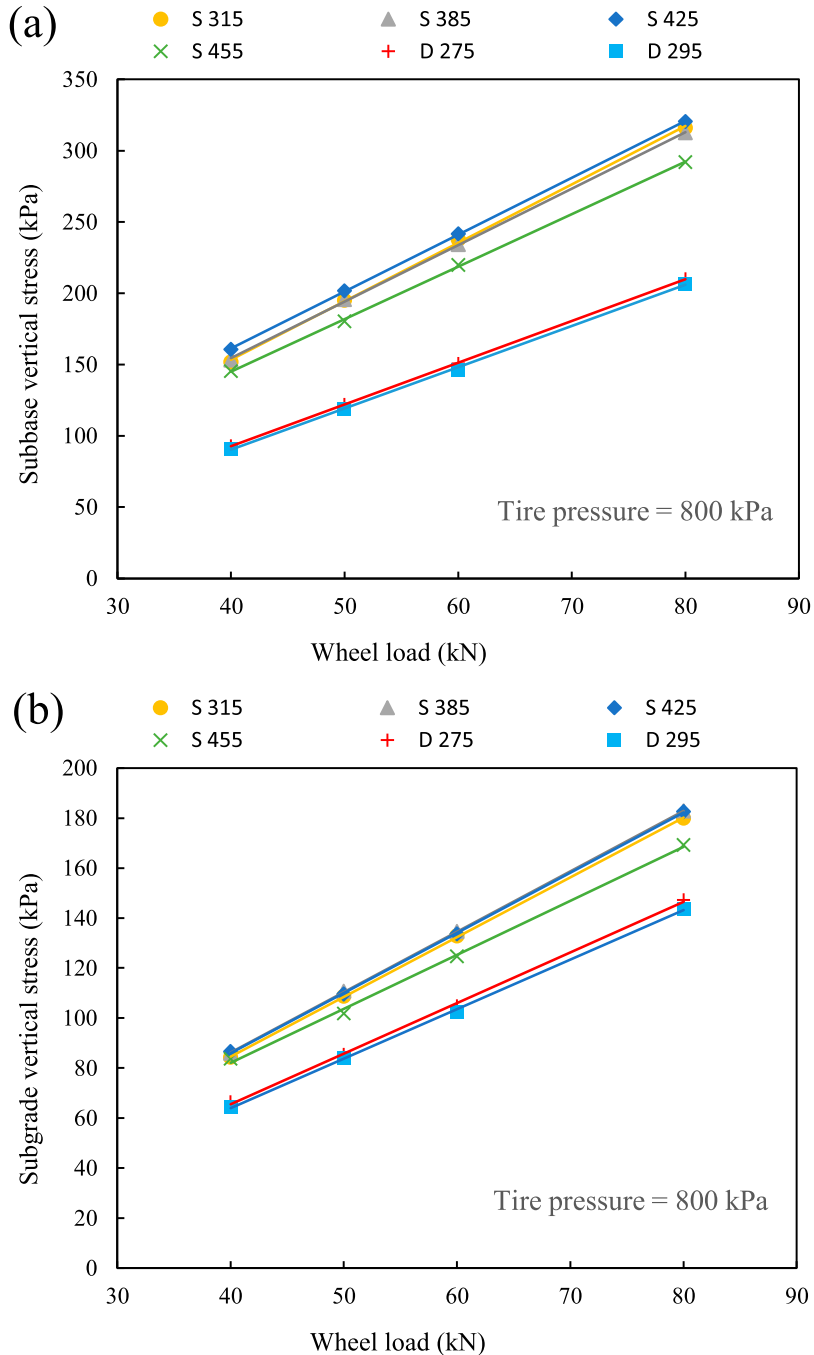

Figure 17. Peak vertical stresses at (a) the top of the subbase, and (b) the upper part of the subgrade with respect to wheel load.

To compare the risks of subgrade rutting associated with the different tires, the same method as for the AC fatigue cracking was followed. The damage ratios (D) for subgrade rutting with respect to the D295 tire are presented in Table 5.

The numbers in Table 5 depict that the single wheels are more damaging to the subgrade than the dual wheels. Among the single wheels, the S455 wheel is the least damaging (D ranged from 1.4–2.0) and the S425 (D ranged from 2.2–3.8) is the most damaging one. Compared to the AC fatigue cracking, the D values are much lower indicating that tire dimensions have a less significant impact on subgrade rutting.

Vertical stresses in unbound layers

Figures 14a–c present the vertical stresses at three depths (z), i.e. at 0.212, 0.453, and 0.603 m, respectively, from the top of the pavement surface. Figure 15 shows the peak stresses disregarding the lateral positions. It is apparent that the dual tires always induced lower stresses than the single tires. At the lower depth of 0.212 m, stresses under the single tires were significantly higher than those under the dual tires. However, the differences diminished with depth as can be seen for the other two depths. The NGWB single tire S455 produced slightly lower vertical stresses compared to the other single tires (probably due to increased contact area, as shown in Table 3) while the FGWB single tire S425 induced the highest stresses.

Figure 16 shows the peak vertical stresses in the subbase and the subgrade with respect to inflation pressure. For the dual tires and the S455 tire, stresses in the subbase and subgrade appeared to be reduced with increased inflation pressure. For the other single tires, stresses increased with increased tire pressure. On the other hand, peak vertical stresses always increased with increased wheel load as seen in Figure 17.

Conclusions

The measurements of this study indicate that compared to dual tires, the single tires induced more longitudinal and transverse stains at the bottom of AC layer and hence pose increased risk of fatigue cracking of the AC layers. Similarly, the single tires produced higher vertical stresses and strains in the unbound base, subbase and subgrade layers and thus increase the risk of permanent deformation in the unbound pavement layers. Among the single tires, the NGWB S455 tire appeared to be the least damaging for the pavement. The FGWB S425 tire was found to be the most damaging one in terms of vertical stress and strain which is consistent with other previous studies (Fedujwar & Sahoo, 2023; Greene et al., 2010; Said et al., 2021). When the relative damages (damage ratios) were compared with respect to the dual D295 tire, it was observed that the other tires can be several times more damaging depending on the type of damage and loading. However, the S455 was significantly less damaging than the other single tires. Considering that NGWB tires can significantly reduce fuel consumption, they can overweigh slightly increased pavement damage compared to dual tires (Al-Qadi et al., 2018; Said et al., 2021).

The impact of wheel load was consistent across all tire types, with stresses and strains increasing proportionally to the load. However, when it comes to the effect of inflation pressure, the S455 tire and the dual tires exhibited similar behaviour. These tires demonstrated a reduction in stresses and strains as inflation pressure increased, whereas the other tires displayed the opposite trend.

The study was conducted on a thin asphalt pavement structure, and the results may be influenced by factors such as layer thickness and other structural properties. Additionally, variations in tire tread patterns, materials, and construction could have impacted the measured responses. It is important to note that the tests were performed under controlled conditions at the HVS facility, which may not fully reflect real-world scenarios where climate and loading conditions can differ. Moreover, the wheel speed at the HVS facility was lower than typical traffic speeds, potentially affecting the observed results. Furthermore, the D values calculated here were assuming $b = -4$ in Equation 1 for all layers.

In reality, this may vary depending on the layer properties and hence should be investigated for more accurate analysis. While the study provides some insight into the relative damage risks posed by different tires, it is recommended that further testing be conducted on structures with varying thicknesses and other types of tires to gain a more comprehensive understanding.

Disclosure statement

Funding

References

Ahmed, A. W., Rahman, M. S., & Erlingsson, S. (2018). *Impact of tire types and configurations on responses of a thin pavement structure*. International Conference on Advances in Materials and Pavement Performance Prediction (AM3P 2018), pp. 271.

Al-Qadi, I. L., Elseifi, M. A., & Yoo, P. J. (2004). *Pavement damage due to different tires and vehicle configurations*. Final report submitted to Michelin Americas Research and Development Corporation.

Al-Qadi, I. L., Hernandez, J. A., Gamez, A., Ziyadi, M., Gungor, O. E., & Kang, S. (2018). Impact of wide-base tyres on pavements: A national study. *Transportation Research Record*, *2672*(40), 186–196. https://doi.org/10.1177/0361198118757969

Al-Qadi, I. L., Loulizi, A., Elseifi, M. A., & Lahouar, S. (2000). *Effect of tire type on flexible pavements response to truck loading*. Final report submitted to Michelin Americas Research and Development Corporation.

Al-Qadi, I. L., & Wang, H. (2009). *Evaluation of pavement damage due to new tire designs. Research report ICT-09-048*. Illinois Center for Transportation, University of Illinois at Urbana-Champaign.

Al-Qadi, I. L., & Wang, H. (2012). Impact of wide-base tires on pavements: Results from instrumentation measurements and modeling analysis. *Transportation Research Record*, *2304*(1), 169–176. https://doi.org/10.3141/2304-19

Bai, T., Cheng, Z., Hu, X., Fuentes, L., & Walubita, L. F. (2021). Viscoelastic modelling of an asphalt pavement based on actual tire-pavement contact pressure. *Road Materials and Pavement Design*, *22*(11), 2458–2477. DOI: 10.1080/14680629.2020.1766545

COST334. (2001). *Effects of wide single tires and dual tires: Final report of the action*. European Cooperation in the Field of Scientific and Technical Research. Brussels, Belgium.

De Beer, M., Fisher, C., & Kannemeyer, L. (2004). *Tire-pavement interface contact stresses on flexible pavements quo vadis?* In Proceedings of the 8th Conference on Asphalt Pavements for Southern Africa (CAPSA'04) (pp. 12-16 September). Sun City, South Africa. ISBN 1-920-01718-6.

Fedujwar, R. R., & Sahoo, U. C. (2023). Pavement responses under wide base tyres subjected to moving loads. *International Journal of Transportation Science and Technology*, *12*(2), 549–559. https://doi.org/10.1016/j.ijtst.2022.05.006

Gong, Z., Miao, Y., Li, W., Yu, W., & Wang, L. (2023). Analysis of tyre-pavement contact behaviour of heavy truck in full-scale test. *International Journal of Pavement Engineering*, *24*(1), 2235630. DOI: 10.1080/10298436.2023.2235630

Greene, J., Toros, U., Kim, S., Byron, T., & Choubane, B. (2010). Impact of wide-base single tires on pavement damage. *Transportation Research Record*, *2155*(1), 82–90. https://doi.org/10.3141/2155-09

Huang, Y. H. (2004). *Pavement analysis and design* (2nd ed.). Prentice Hall.

Liu, Q., Pei, J., Wang, Z., Hu, D., Huang, G., Meng, Y., Lyu, L., & Zheng, F. (2024). Analysis of tire-pavement interaction modeling and rolling energy consumption based on finite element simulation. *Construction and Building Materials*, *425*, 136101. https://doi.org/10.1016/j.conbuildmat.2024.136101

Manyo, E. Y., Reynaud, P., Picoux, B., Tautou, R., Nelias, D., Allou, F., & Petit, C. (2021). Towards fast modelling of the tire-pavement contact. *European Journal of Environmental and Civil Engineering*, *25*(13), 2396–2412. DOI: 10.1080/19648189.2019.1628812

Moazami, D., Muniandy, R., Hamid, H., & Yusoff, Z. M. (2011). Effect of tire footprint area in pavement response studies. *International Journal of Physical Sciences*, *6*(21), 5040–5047. https://doi.org/10.5897/IJPS11.1085

Saevarsdottir, T., Erlingsson, S., & Carlsson, H. (2016). Instrumentation and performance modelling of heavy vehicle simulator tests. *International Journal of Pavement Engineering*, *17*(2), 148–165. https://doi.org/10.1080/10298436.2014.972957

Said, S., Ahmed, A., Jelagin, D., Lu, X., Gudmarsson, A., Nilsson, R., Oscarsson, E., & Jarlsson, H. (2020). *Prediction of rutting in asphalt concrete pavements – the PEDRO model*. VTI rapport 1016A. Statens väg- och transportforskningsinstitut (VTI)

Said, I., Okte, E., Hernandez, J., & Al-Qadi, I. L. (2021). Impact of new generation wide-base tires on fuel consumption. *Journal of Transportation Engineering, Part B: Pavements*, *147*(2), 04021011. https://doi.org/10.1061/jpeodx.0000266

Saliko, D., & Erlingsson, S. (2021). Damage investigation of thin flexible pavements to longer heavier vehicle loading through instrumented road sections and numerical calculations. *Road Materials and Pavement Design*, *22*(sup1), S575–S591. DOI: 10.1080/14680629.2021.1899964

Saliko, D., & Erlingsson, S. (2023). Evaluation of the structural response of two in-service thin flexible pavements under heavy vehicle loading during different seasons by built-in sensors. *International Journal of Pavement Engineering*, *24*(2), 2138875. DOI: 10.1080/10298436.2022.2138875

Wang, H., Al-Qadi, I. L., & Stanciulescu, I. (2012). Simulation of tyre–pavement interaction for predicting contact stresses at static and various rolling conditions. *International Journal of Pavement Engineering*, *13*(4), 310–321. DOI: 10.1080/10298436.2011.565767

Wang, G., & Roque, R. (2011). Impact of wide-based tires on the near-surface pavement stress states based on a three-dimensional tire-pavement interaction model. *Road Materials and Pavement Design*, *12*(3), 639–662. https://doi.org/10.1080/14680629.2011.9695264

Wiman, L. G. (2006). *Accelerated load testing of pavements: HVS-NORDIC tests at VTI Sweden 2003-2004,* VTI report 544A.

Wiman, L. G., & Erlingsson, S. (2008). *Accelerated pavement testing by HVS – a trans-national testing equipment*. Transport Research Arena Europe 2008, Ljubljana, 21-24 April.

Wollny, I., Behnke, R., Villaret, K., & Kaliske, M. (2016). Numerical modelling of tyre–pavement interaction phenomena: Coupled structural investigations. *Road Materials and Pavement Design*, *17*(3), 563–578. DOI: 10.1080/14680629.2015.1094399

Xie, Y., & Yang, Q. (2019). Tyre–pavement contact stress distribution considering tyre types. *Road Materials and Pavement Design*, *20*(8), 1899–1911. DOI: 10.1080/14680629.2018.1473285

Xue, W., & Weaver, E. (2015). Influence of tyre configuration on pavement response and predicted distress. *International Journal of Pavement Engineering*, *16*(6), 538–548. DOI: 10.1080/10298436.2014.943206

Xue, W., Weaver, E., Wang, L., & Wang, Y. (2016). Influence of tyre inflation pressure on measured pavement strain responses and predicted distresses. *Road Materials and Pavement Design*, *17*(2), 328–344. DOI: 10.1080/14680629.2015.1080180

Zhao, J., & Wang, H. (2022). Dynamic pavement response analysis under wide-base tyre considering vehicle-tyre–pavement interaction. *Road Materials and Pavement Design*, *23*(7), 1650–1666. DOI: 10.1080/14680629.2021.1910551

Zheng, B., Chen, J., Zhao, R., Tang, J., Tian, R., Zhu, S., & Huang, X. (2022). Analysis of contact behaviour on patterned tire-asphalt pavement with 3-D FEM contact model. *International Journal of Pavement Engineering*, *23*(2), 171–186. DOI: 10.1080/10298436.2020.1736294